

Azo-dye-structure dependence of photoinduced anisotropy observed in PMMA films

Keiko Tawa^{a,b,*}, Kenji Kamada^b, Koji Ohta^b

^a Fields and Reactions, PRESTO, JST, Japan

^b Osaka National Research Institute, AIST, MITI, Ikeda, Osaka 563-8577, Japan

Received 25 November 1999; received in revised form 16 February 2000; accepted 8 March 2000

Abstract

Polarized light-induced anisotropy of 4-dimethylamino-4'-nitroazobenzene (DMANA; $\text{NO}_2\text{-C}_6\text{H}_4\text{-N=N-C}_6\text{H}_4\text{-N(CH}_3)_2$) in PMMA is investigated by polarized spectroscopy and compared with the anisotropy of Disperse Orange 3 (DO3; $\text{NO}_2\text{-C}_6\text{H}_4\text{-N=N-C}_6\text{H}_4\text{-NH}_2$) studied previously. The orientation factors evaluated from spectroscopic results show that the *trans* isomers of DMANA isomerize to *cis* forms by motion of the *p*- $\text{NO}_2\text{-C}_6\text{H}_4$ group easily compared with motion of the *p*- $\text{N(CH}_3)_2\text{-C}_6\text{H}_4$ group. This result is different from the result of DO3 in PMMA where the *trans* forms tend to isomerize to *cis* forms by motion of the amino group side than that of nitro group side. We consider that this difference is due to the volume effect of the substituent at the *para* position of a phenyl group. This study clearly indicates that the motion of push-pull azo-dyes in the isomerization processes strongly depends on the relative volume of the *p*-substituent. © 2000 Elsevier Science S.A. All rights reserved.

Keywords: Photoinduced anisotropy; Push-pull azo-dyes; PMMA; *p*-Substituent; Polarized FT-IR; Orientation factors

1. Introduction

Azobenzenes with both electron donor (D) and acceptor (A) have attracted the interest of a large number of researchers in the field of photonics. This push-pull type of azo-dyes has a larger polarity than that of an azobenzene without a substituent, and the *cis* molecule of push-pull azobenzenes formed via the photoisomerization process can thermally reisomerize to the *trans* molecule quickly [1] because of large charge separation induced by D and A. The large polarity and the fast reisomerization (thermal isomerization) lead push-pull azo-dyes towards becoming prospective new optical functional materials utilizing the second-order nonlinear optical effect [2,3] or polarized light-induced anisotropy [4–7,24,25].

A polarized light-induced anisotropy [4–7,24,25] has been observed in polymer films doped with photochromic molecules. Since the 1980s, this type of anisotropy has been studied in polymers doped with azo-dyes for transient polarization holography by Todorov and co-workers [8,9]. Then, polarized light-induced anisotropy has also been examined in the mixture of azo-dyes and liquid crystals

[10,11,26–28], and it has been expected as being a new optical switching material. In the mixture of azo-dyes and liquid crystals, the orientation of azo-dyes induced by irradiating the polarized light can be a driving force for alignment of the liquid crystals. While the technology for the application to various optical devices has been advanced, studying the dynamics of azo-dyes during photoisomerization or thermal isomerization processes is essential for the comprehension of the physical mechanisms for photoinduced anisotropy.

We have studied the matrix-dependence of photoinduced anisotropy [12]. The molecular motion of push-pull azo-dyes has been evaluated by orientation factors which were obtained from polarized UV-VIS and FT-IR spectroscopies [13,14]. Disperse Orange 3 (DO3, $\text{NO}_2\text{-C}_6\text{H}_4\text{-N=N-C}_6\text{H}_4\text{-NH}_2$) was used in our previous studies. In most polymer matrices such as methacrylate polymers and polystyrene, the *trans* forms of DO3 tend to isomerize to *cis* forms by the motion of the *p*- $\text{NH}_2\text{-C}_6\text{H}_4$ group side, because the relative volume of the *p*- $\text{NH}_2\text{-C}_6\text{H}_4$ group is considered to be small compared to that of the *p*- $\text{NO}_2\text{-C}_6\text{H}_4$ group.

In this paper, we also use another push-pull azo-dye, 4-dimethylamino-4'-nitro azobenzene (DMANA, $\text{NO}_2\text{-C}_6\text{H}_4\text{-N=N-C}_6\text{H}_4\text{-N(CH}_3)_2$) having an amino group of a larger volume in order to examine the relationship between

* Corresponding author. Tel.: +81-727-51-9523; fax: +81-727-51-9637. E-mail address: keiko-o@onri.go.jp (K. Tawa)

the relative volume of *p*-substituents and the motion of azo molecules during the isomerization process. The absorption peak (wavelength: λ_{\max}) which corresponds to $\pi\pi^*$ transition of the *trans* isomer appears at a longer wavelength than that of DO3 because of the stronger electron donor of DMANA. The molecular structure dependence of photoinduced anisotropy is anticipated to help us understand the molecular motion of azo-dye in the photoisomerization process induced by polarized light. For this purpose, the comparison of dynamic behavior between DO3 and DMANA is made by polarized UV–VIS and FT-IR spectroscopies.

2. Experimental

2.1. Samples

Push–pull azo-dyes, DMANA (Tokyo Kasei) and DO3 (Aldrich), were used as photochromic molecules. Poly(methyl methacrylate) (PMMA, Aldrich, $M_w=120,000$, $T_g\sim 114^\circ\text{C}$) was used as a matrix. The cast film of PMMA doped with each dye was prepared from a chloroform solution. The thickness of the films was less than 20 μm . The dye concentration was about 1 wt.%. The films were annealed at 90°C for several hours. The residual chloroform in the prepared films was measured by FT-IR spectroscopy. The content of residual chloroform was found to be so little that it would have no influence on the photoinduced anisotropy in any of the films.

2.2. Measurements

Linearly polarized continuous-wave light (488 nm) from an Ar ion laser (Spectra-Physics Model 161C) was used as the excitation light. Polarized UV–VIS spectra and polarized FT-IR spectra were taken in the parallel (*Z*) and perpendicular (*Y*) directions to the polarization direction of the Ar ion laser. The optical power of the Ar ion laser was 6 mW cm^{-2} at the sample position in both spectroscopic measurements.

The variations in UV–VIS absorbance along the *Z*- and the *Y*-direction, $E_Z(\lambda)$ and $E_Y(\lambda)$, were measured at λ_{\max} by a Shimadzu UV-2500PC spectrometer. The measurements were performed before irradiation, during irradiation, and after irradiation with polarized excitation light at room temperature (23°C). Before irradiation, all the azo molecules are considered to exist in *trans* isomers. In push–pull azo-dyes, it has been known that the absorption peaks at λ_{\max} in the visible range correspond to the $\pi\pi^*$ transition of the *trans* isomer. The mole fraction of *trans* isomers, α , can be obtained with $(E_Z(\lambda_{\max}) + 2E_Y(\lambda_{\max}))/3$, because the linearly polarized light induces optical anisotropy in the film plane.

The FT-IR spectra of the azo-doped PMMA films were also measured at room temperature (23°C). The spectra were recorded by using a Bio-Rad FTS-175C IR spectrometer equipped with an MCT detector. The wavenumber resolution

was 4 cm^{-1} . The IR spectra of the azo-dyes in the PMMA were obtained by subtracting the spectrum of a blank film from that of dye-doped films. Polarized FT-IR spectra were obtained using the polarizer (KRS-5). All interferograms were collected for every 10 s before irradiation, during irradiation, and after irradiation of the linearly polarized excitation light.

3. Analysis

Orientation factor is useful in discussing statistically averaged alignment of molecules [14]. It is also suitable to analyze the orientation of two isomers of azo-dyes formed by the polarized-light irradiation. We have established the method for determining the orientation factor of the two isomers as reported in our previous study [13]. The process of determination is briefly explained here.

The absorption probability of a band (*a*) along the *Z*-axis in the laboratory-fixed co-ordinates ($F=X, Y, Z$) can be represented by

$$\langle (\mathbf{e}_Z \cdot \mathbf{M}(a))^2 \rangle = M_x^2(a) \langle \cos^2 \theta_x \rangle + M_y^2(a) \langle \cos^2 \theta_y \rangle + M_z^2(a) \langle \cos^2 \theta_z \rangle \quad (1)$$

where \mathbf{e}_Z is a unit vector of the *Z*-polarized light, and $\mathbf{M}(a)$ is an electric dipole transition moment which is represented by components $M_f(a)$ in the molecular-fixed co-ordinates ($f=x, y, z$). The terms of $M_f^2(a) \langle \cos^2 \theta_f \rangle$ ($\langle \rangle$: the statistical average) correspond to the square of the projection of the *f*-components of $\mathbf{M}(a)$ onto the *Z*-axis (Fig. 1), and the off-diagonal terms like $M_x(a)M_y(a) \langle \cos \theta_x \cos \theta_y \rangle$ may vanish by selecting the appropriate system of molecular-fixed co-ordinates which coincide with the molecular orientation axes. The averaged square cosine θ_f is defined as the orientation factor K_{Zf} :

$$K_{Zf} = \langle \cos^2 \theta_f \rangle. \quad (2)$$

The *F*-components of the observed absorbance vector in the laboratory-fixed axes $E_F(a)$ can be represented by

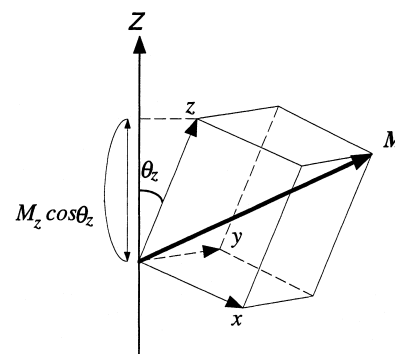


Fig. 1. Projection of the *z*-component of transition moment \mathbf{M} expressed in the molecular axes.

the sum of each matrix element K_{Ff} multiplied by the f -components of the absorbance vector $A_f(a)$ in a molecular framework:

$$E_F(a) = \sum_f K_{Ff} A_f(a) = K_{Fx} A_x(a) + K_{Fy} A_y(a) + K_{Fz} A_z(a). \quad (3)$$

In this study, the sample is considered to have a uniaxial orientation, i.e. $E_X(a) = E_Y(a)$, since the linearly Z-polarized light was used for the source of irradiation and the molecules are selectively excited by the Z-polarized light. Therefore, the matrix K can be described as

$$K = \begin{pmatrix} K_{Xx} & K_{Xy} & K_{Xz} \\ K_{Yx} & K_{Yy} & K_{Yz} \\ K_{Zx} & K_{Zy} & K_{Zz} \end{pmatrix} = \begin{pmatrix} \frac{1 - K_{Zx}}{2} & \frac{1 - K_{Zy}}{2} & \frac{1 - K_{Zz}}{2} \\ \frac{1 - K_{Zx}}{2} & \frac{1 - K_{Zy}}{2} & \frac{1 - K_{Zz}}{2} \\ K_{Zx} & K_{Zy} & K_{Zz} \end{pmatrix}. \quad (4)$$

Azo molecules as used in this study can take two isomeric forms, *trans* and *cis* isomers. So the F -component of the observed absorbance of a vibrational band (a), $E_F(a)$, can be expressed as the sum of the absorbance of two isomers using the mole fraction of the *trans* isomer, α :

$$E_F(a) = \alpha \sum_f K_{Ff}^{(t)} A_f(a)^{(t)} + (1 - \alpha) \sum_f K_{Ff}^{(c)} A_f(a)^{(c)}. \quad (5)$$

The orientation factors for each isomer can be estimated by solving the above simultaneous equations for several different bands.

4. Results and discussion

4.1. Thermal isomerization

The direction of the $\pi\pi^*$ transition moment of the *trans* isomer is known to be almost parallel to the molecular long axis [15,16,29]. As shown in Fig. 2, λ_{\max} in DMANA/PMMA is observed at 486 nm and that in DO3/PMMA is at 438 nm. In the case of push-pull azo-dyes, such a spectral difference in λ_{\max} has been known to reflect the difference in the strength of an electron donor [17] which leads to the difference in polarity. Here, the dimethylamino group is a stronger electron donor than the amino group of DO3.

The mole fraction of the *trans* isomer during the isomerization process, α , can also be obtained by monitoring the absorbance at λ_{\max} and normalizing it to the initial absorbance before irradiation as the mole extinction coefficient (ϵ) for the *trans* isomers at λ_{\max} is about 25 times larger than that for the *cis* isomers [18]. If the mole fraction of the

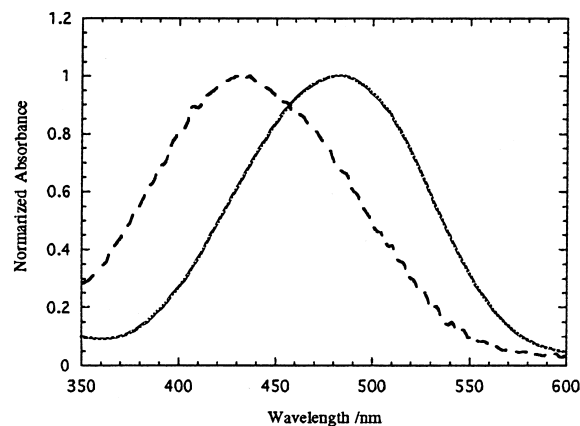


Fig. 2. UV-VIS spectra of DMANA (—) and DO3 (---) doped in PMMA films.

trans forms is 0.8, the contribution of the *cis* isomers to the absorbance at λ_{\max} is less than 0.01 ($= (0.2 \times 0.04) / (0.8 \times 1)$) and it can be neglected in determining the α -value in this study. The α -values began to decrease upon irradiation and reached a constant value, which exhibits the photostationary state. The α -values in the photostationary state were 0.83 (DMANA) and 0.82 (DO3). On turning the light off, the α -values increased and finally recovered to 1. The variations of absorbance are shown in Fig. 3. The reversion (thermal isomerization) time τ_{ct} is defined by an empirical technique [19], i.e. as the time such that 90% of the *cis* isomers convert to *trans* isomers at a convenient estimate. τ_{ct} for DMANA was about 30 s, which was shorter than that for DO3 (ca. 70 s). For the push-pull azo-dyes in any solvent, *cis* molecules generally isomerize not only via slow inversion processes but also by rapid rotation processes because the azo-dye with a stronger electron donor promotes charge separation in a molecule [18,20,30]. The fact of faster reversion for DMANA as well as the result of the red-shift of λ_{\max} support that the molecule has a larger polarity than that for DO3.

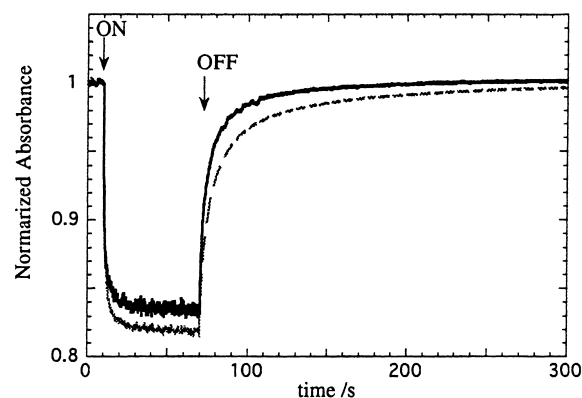


Fig. 3. The variation of absorbance at λ_{\max} in UV-VIS spectra when the Ar ion laser was turned on and off: DMANA (—) and DO3 (---).

Table 1

Absorbances in a photostationary state, $E_Z(\lambda_{\max})$ and $E_Y(\lambda_{\max})$, and the anisotropy ratio calculated by $(E_Z(\lambda_{\max}) - E_Y(\lambda_{\max})) / (E_Z(\lambda_{\max}) + 2E_Y(\lambda_{\max}))$

	DO3	DMANA
$E_Z(\lambda_{\max})$	0.71	0.72
$E_Y(\lambda_{\max})$	0.87	0.88
Anisotropy ratio	-0.065	-0.065

4.2. Polarized light-induced anisotropy

In the cases of DMANA and DO3, the *cis* isomer formed by irradiation has little visible absorption around each λ_{\max} of the *trans* isomer [1,18]. Therefore, polarized-light induced anisotropy for the *trans* isomer can be estimated with $E_Z(\lambda_{\max})$ and $E_Y(\lambda_{\max})$ in the visible range. Anisotropy ratios for the *trans* isomers are calculated by $(E_Z(\lambda_{\max}) - E_Y(\lambda_{\max})) / (E_Z(\lambda_{\max}) + 2E_Y(\lambda_{\max}))$. As shown in Table 1, the anisotropy ratio is almost the same between DMANA and DO3. However, anisotropy for the *cis* isomers cannot be obtained by this method.

Figs. 4 and 5 show the polarized infrared spectra of DMANA and DO3 in PMMA, respectively, before irradiation and during irradiation in the wavenumber range of 1650–1280 cm^{-1} . Three vibrational bands are assigned to symmetric (NO_2^s , 1340 cm^{-1} (DMANA) and 1341 cm^{-1} (DO3)) and antisymmetric (NO_2^{as} , 1523 cm^{-1} (DMANA) and 1523 cm^{-1} (DO3)) stretching modes of NO_2 , and the C–N stretching mode of C-amino (C–N, 1311 cm^{-1}

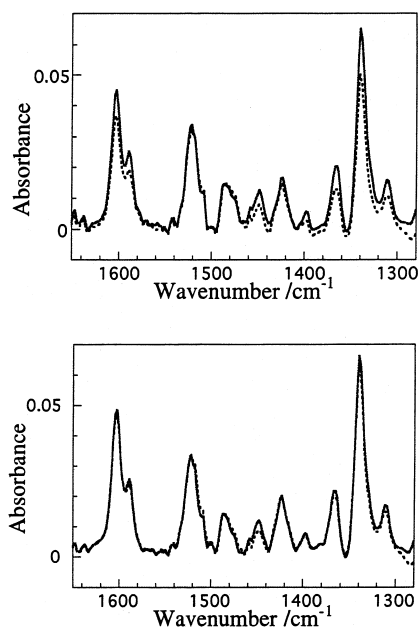


Fig. 4. Polarized FT-IR spectra of DMANA in PMMA (subtraction spectra): upper panel (Z-direction) and lower panel (Y-direction), before irradiation (—) and during irradiation (---).

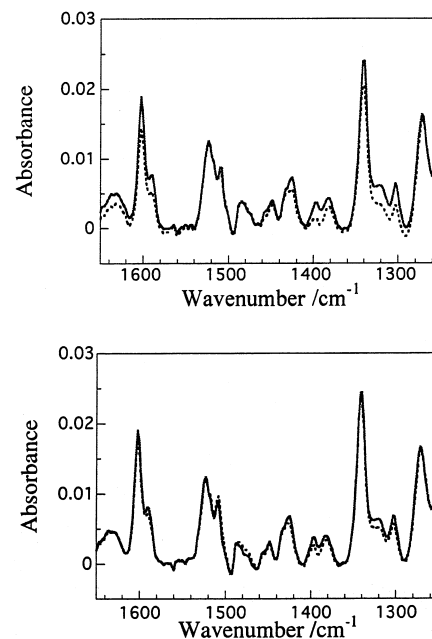


Fig. 5. Polarized FT-IR spectra of DO3 in PMMA (subtraction spectra): upper panel (Z-direction) and lower panel (Y-direction), before irradiation (—) and during irradiation (---).

(DMANA) and 1303 cm^{-1} (DO3)) [21,22]. Using the NO_2^s , NO_2^{as} and C–N bands, Eq. (5) explained in Section 3 was used for determining the orientation factors. From polarized FT-IR spectra, the six data, $E_Z(\text{NO}_2^s)$, $E_Z(\text{NO}_2^{as})$, $E_Z(\text{C–N})$, $E_Y(\text{NO}_2^s)$, $E_Y(\text{NO}_2^{as})$, and $E_Y(\text{C–N})$ were utilized. α was obtained by UV–VIS absorption.

In order to determine the orientation factors, we defined the molecular-fixed co-ordinates for the *trans* and *cis* isomers, as shown in Fig. 6a and b, respectively [13]. The absorbance in this molecular framework can be determined as

$$\mathbf{A}(\text{NO}_2^s)^{(t)} = \begin{pmatrix} A_x(\text{NO}_2^s)^{(t)} \\ A_y(\text{NO}_2^s)^{(t)} \\ A_z(\text{NO}_2^s)^{(t)} \end{pmatrix} = \begin{pmatrix} 0 \\ 0 \\ A_z(\text{NO}_2^s)^{(t)} \end{pmatrix},$$

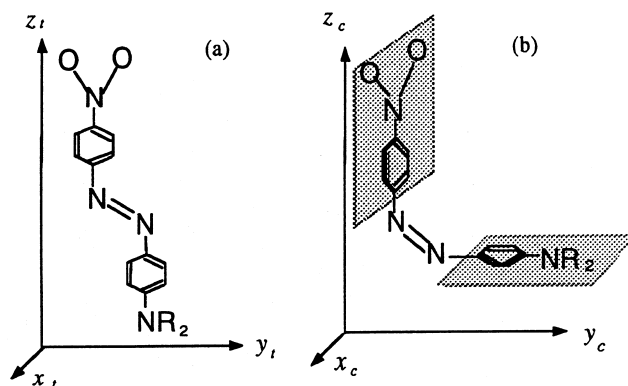


Fig. 6. Molecular axes for a (a) *trans* isomer and a (b) *cis* isomer: R=H (DO3), CH_3 (DMANA).

$$\mathbf{A}(\text{NO}_2^{as})^{(t)} = \begin{pmatrix} A_x(\text{NO}_2^{as})^{(t)} \\ A_y(\text{NO}_2^{as})^{(t)} \\ A_z(\text{NO}_2^{as})^{(t)} \end{pmatrix} = \begin{pmatrix} 0 \\ A_y(\text{NO}_2^{as})^{(t)} \\ 0 \end{pmatrix},$$

$$\mathbf{A}(\text{C-N})^{(t)} = \begin{pmatrix} A_x(\text{C-N})^{(t)} \\ A_y(\text{C-N})^{(t)} \\ A_z(\text{C-N})^{(t)} \end{pmatrix} = \begin{pmatrix} 0 \\ 0 \\ A_z(\text{C-N})^{(t)} \end{pmatrix},$$

$$\mathbf{A}(\text{NO}_2^s)^{(c)} = \begin{pmatrix} A_x(\text{NO}_2^s)^{(c)} \\ A_y(\text{NO}_2^s)^{(c)} \\ A_z(\text{NO}_2^s)^{(c)} \end{pmatrix} = \begin{pmatrix} 0 \\ 0 \\ A_z(\text{NO}_2^s)^{(c)} \end{pmatrix},$$

$$\mathbf{A}(\text{NO}_2^{as})^{(c)} = \begin{pmatrix} A_x(\text{NO}_2^{as})^{(c)} \\ A_y(\text{NO}_2^{as})^{(c)} \\ A_z(\text{NO}_2^{as})^{(c)} \end{pmatrix} = \begin{pmatrix} A_x(\text{NO}_2^{as})^{(c)} \\ 0 \\ 0 \end{pmatrix},$$

$$\mathbf{A}(\text{C-N})^{(c)} = \begin{pmatrix} A_x(\text{C-N})^{(c)} \\ A_y(\text{C-N})^{(c)} \\ A_z(\text{C-N})^{(c)} \end{pmatrix} = \begin{pmatrix} 0 \\ A_y(\text{C-N})^{(c)} \\ 0 \end{pmatrix}. \quad (6)$$

The orientation factors for each isomer can be estimated by solving the simultaneous equations for three bands as shown by

$$E_F(\text{NO}_2^s) = \alpha \sum_f K_{Ff}^{(t)} A_f(\text{NO}_2^s)^{(t)} + (1 - \alpha) \sum_f K_{Ff}^{(c)} A_f(\text{NO}_2^s)^{(c)},$$

$$E_F(\text{NO}_2^{as}) = \alpha \sum_f K_{Ff}^{(t)} A_f(\text{NO}_2^{as})^{(t)} + (1 - \alpha) \sum_f K_{Ff}^{(c)} A_f(\text{NO}_2^{as})^{(c)},$$

$$E_F(\text{C-N}) = \alpha \sum_f K_{Ff}^{(t)} A_f(\text{C-N})^{(t)} + (1 - \alpha) \sum_f K_{Ff}^{(c)} A_f(\text{C-N})^{(c)}. \quad (7)$$

Molecular axes for the *trans* isomer were chosen so that the molecule takes a planar structure in the y_t - z_t plane. The relationship $K_{Zx}^{(t)} = K_{Zy}^{(t)}$ can be assumed since the direction of the $\pi\pi^*$ transition moment is parallel to the z_t -axis in the present molecular framework. The *cis* molecule is assumed to take a structure with the two phenyl ring planes perpendicular to each other as shown in Fig. 6b. It was shown in the previous paper [13] that this assumption can be justified with the result that the orientation factors so-determined are almost the same whenever *p*-NO₂-C₆H₄ is a z_c - y_c or a z_c - x_c plane.

The $K_{Zz}^{(t)}$ and $K_{Zf}^{(c)}$ ($f: x, y, z$) obtained here are shown in Fig. 7a-d. In Fig. 7a and b, $K_{Zz}^{(t)}$ -values in the *trans* isomers should be 1/3 when the system is isotropic. For both the azo-dyes, the $K_{Zz}^{(t)}$ -values are smaller than 1/3 during irradiation, and they will recover to 1/3 on turning the light off. This means that the *trans* isomers with a small angle

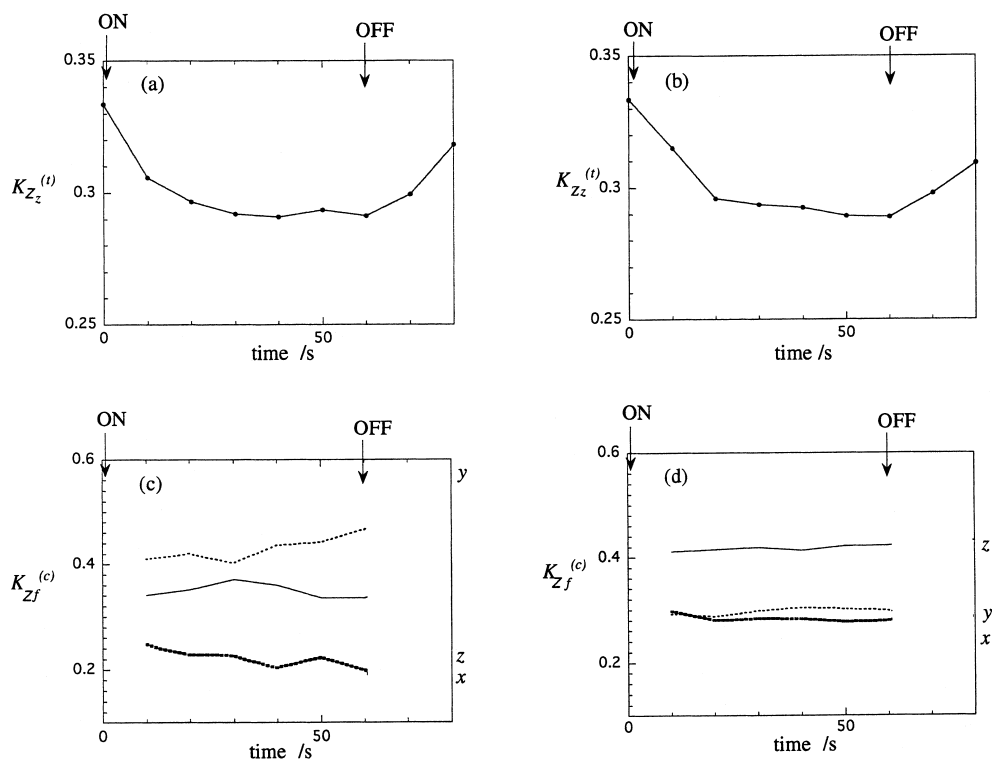


Fig. 7. Orientation factors: (a) $K_{Zz}^{(t)}$ of DMANA (*trans*); (b) $K_{Zz}^{(t)}$ of DO3 (*trans*); (c) $K_{Zf}^{(c)}$ of DMANA (*cis*) and (d) $K_{Zf}^{(c)}$ of DO3 (*cis*).

between the *Z*- and the z_t -axis were excited selectively by linearly *Z*-polarized light. The $K_{Zz}^{(t)}$ -value in DMANA/PMMA was almost the same as that in DO3/PMMA, i.e. the anisotropy was almost the same between them (Fig. 7a and b). The result is also consistent with the fact that the anisotropy ratio for DMANA obtained from polarized UV–VIS spectroscopy was almost the same as that of DO3, as shown in Table 1. $K_{Zz}^{(t)}$ is theoretically equal to $(2r+1)/3$, where r (the anisotropy ratio) is estimated by $(E_Z(\lambda_{\max}) - E_Y(\lambda_{\max})) / (E_Z(\lambda_{\max}) + 2E_Y(\lambda_{\max}))$ obtained from polarized UV–VIS spectroscopy. The equality is shown in two experimental values, $K_{Zz}^{(t)}$ and r , in this study. The rotational motion of *trans* isomers is considered to be restricted within a small free volume of PMMA [23,31,32].

For the *cis* isomer, the $K_{Zf}^{(c)}$ -value is indefinite at the initial stage (time: 0) because there is no *cis* molecule before irradiation. Twenty seconds after turning the laser light off, the mole fraction of the *cis* isomers for DMANA is less than 2% as shown in Fig. 3. Comparison of the orientation factors for the *cis* isomers between DMANA and DO3 is not considered to be reliable because of the experimental error obtained by a low concentration of the *cis* isomers. Therefore, the data after turning the light off are omitted for the *cis* isomer (Fig. 7c and d). The $K_{Zf}^{(c)}$ -value is defined as an average value by $\langle \cos^2 \theta_f \rangle$ as written in Section 3. $K_{Zf}^{(c)}$ is considered to reflect the averaged motion of azo molecules in the photoisomerization process. A *trans* molecule which has the transition moment parallel to the polarization direction of the laser light is excited selectively. If the *trans* molecule isomerizes without fixing a specific side into the molecule or the rate of the rotational diffusion of a molecule is very fast even in the polymer like in solvents, the *cis* molecules are never oriented towards a certain direction and anisotropy is not observed. However, we observed the polarized light-induced anisotropy of the *cis* forms. Therefore, the molecule is considered to isomerize to the *cis* form by the motion of the mobile side, i.e. (i) the *p*-NO₂-C₆H₄ side (amino side is fixed), (ii) the *p*-NR₂-C₆H₄ side (NO₂ side is fixed), and (iii) both phenyl sides (N=N is fixed). In each hypothesis, the magnitude of $K_{Zf}^{(c)}$ -values is as: (i) $K_{Zy}^{(c)} \gg K_{Zz}^{(c)}, K_{Zx}^{(c)}$, (ii) $K_{Zz}^{(c)} \gg K_{Zy}^{(c)}, K_{Zx}^{(c)}$, (iii) $K_{Zz}^{(c)} = K_{Zy}^{(c)} > K_{Zx}^{(c)}$.

During irradiation, in the case of DMANA, the $K_{Zy}^{(c)}$ -values became larger than the $K_{Zx}^{(c)}$ - and $K_{Zz}^{(c)}$ -values in PMMA (Fig. 7c). The larger $K_{Zy}^{(c)}$ -values indicate that there are a large number of *cis* molecules with a small angle between the *Z*- and the y_c -axis. In other words, in the *cis* form, *p*-N(CH₃)₂-C₆H₄ has the tendency to align with *Z*-axis by motion of the NO₂ group side in the isomerization process. On the other hand, in the case of DO3/PMMA, the $K_{Zz}^{(c)}$ -values were found to be the largest of the three orientation factors for *cis* isomers (Fig. 7d). The larger $K_{Zz}^{(c)}$ means that, in the *cis* form, *p*-NO₂-C₆H₄ tends to align with the *Z*-axis by motion of the NH₂ group side. From these results, we can consider that the *p*-NO₂-C₆H₄ group of

DMANA is more mobile than the *p*-N(CH₃)₂-C₆H₄ group. In the case of DO3, the *p*-NH₂-C₆H₄ group tends to move and the *p*-NO₂-C₆H₄ group does not move so easily. This difference in behavior between DMANA and DO3 is probably due to difference in the volume of *p*-substituents. Thus, the motion of push–pull azo molecules is found to strongly depend on the molecular structure of azo-dyes. Such results can be understood by using polarized spectroscopic techniques including the orientation factors as discussed here.

5. Conclusion

Push–pull azo-dyes are promising materials for new optical switching elements, and in the substrates for liquid crystal cell, films attached to azo-dyes can be utilized. In spite of the important compounds, the relationships between the molecular structure and the orientational behavior have not been clarified sufficiently. In this study, the polarized light-induced anisotropy of DMANA and DO3 molecules was measured by polarized UV–VIS and FT-IR spectroscopies. Comparing the molecular structure of DMANA with that of DO3, the structure of the two dyes is similar except for the substituent at the *para* position of a phenyl group, i.e. the N(CH₃)₂ group for DMANA and the NH₂ group for DO3. The anisotropies for *trans* forms were found to be almost the same between DMANA and DO3. On the contrary, the molecular orientation behavior for the *cis* isomers of DMANA is found to be different from that of DO3 from the orientation factors obtained from the polarized FT-IR measurement. It was found that more DMANA molecules can isomerize by the motion of the *p*-NO₂-C₆H₄ group than by the motion of the *p*-N(CH₃)₂-C₆H₄ group. On the other hand, a large number of DO3 molecules can isomerize by the motion of the *p*-NH₂-C₆H₄ group than that of the *p*-NO₂-C₆H₄ group. We consider that the result is due to the relative volume between two *p*-substituents. This study clarified the relationship between the orientational behavior of *cis* forms and the molecular structure of azo-dyes. The motion of push–pull azo molecules strongly depends on the molecular structure of azo-dyes.

References

- [1] H. Rau, in: J.F. Rabek (Ed.), Photochemistry and Photophysics, Vol. 2, CRC, Boca Raton, FL, 1990 (Chapter 4).
- [2] G.A. Lindsay, K.D. Singer (Eds.), Polymers for Second-order Nonlinear Optics, ACS Symposium Series 601, American Chemical Society, Washington, DC, 1995.
- [3] S. Miyata, H. Sasabe (Eds.), Advances in Nonlinear Optics, Vol. 4, Poled Polymers and Their Applications to SHG and EO Devices, Gordon and Breach, Amsterdam, 1997.
- [4] G.S. Kumar, D.C. Neckers, Chem. Rev. 89 (1989) 1915.
- [5] S. Xie, A. Natansohn, P. Rochon, Chem. Mater. 5 (1993) 403.
- [6] Z. Sekkat, M. Dumont, Appl. Phys. B 53 (1991) 121.
- [7] Y. Yamaguchi, T. Okamoto, O. Urakawa, Q. Tran-Cong, Polym. J. 30 (1998) 414.

- [8] T. Todorov, L. Nikolova, N. Tomova, V. Dragostinova, *Opt. Quantum Electron.* 13 (1981) 209.
- [9] V. Mateev, P. Markovsky, L. Nikolova, T. Todorov, *J. Phys. Chem.* 96 (1992) 3055.
- [10] T. Ikeda, T. Sasaki, K. Ichimura, *Nature* 361 (1993) 428.
- [11] S. Hvilsted, F. Andruzzi, P.S. Ramanujam, *Optics Lett.* 17 (1992) 1234.
- [12] K. Tawa, K. Kamada, T. Sakaguchi, K. Ohta, *Polymer* 41 (2000) 3235.
- [13] K. Tawa, K. Kamada, T. Sakaguchi, K. Ohta, *Appl. Spectrosc.* 52 (1998) 1356.
- [14] J. Michl, E.W. Thulstrup (Eds.), *Spectroscopy with Polarized Light*, VCH, New York, 1986.
- [15] J.G. Radziszewski, J. Michl, *J. Am. Chem. Soc.* 108 (1986) 3289.
- [16] D.L. Beveridge, H.H. Jaffé, *J. Am. Chem. Soc.* 88 (1966) 1948.
- [17] G.F. Svatos, C. Curran, J.V. Quagliano, *J. Am. Chem. Soc.* 77 (1955) 6159.
- [18] P.D. Wildes, J.G. Pacifici, G. Irick Jr., D.G. Whitten, *J. Am. Chem. Soc.* 93 (1971) 2004.
- [19] A. Natansohn, P. Rochon, J. Gosselin, S. Xie, *Macromolecules* 25 (1992) 2268.
- [20] T. Asano, T. Okada, K. Shinkai, S. Shigematsu, Y. Kusano, O. Manabe, *J. Am. Chem. Soc.* 103 (1981) 5161.
- [21] A. Natansohn, P. Rochon, M. Pezolet, P. Audet, D. Brown, S. To, *Macromolecules* 27 (1994) 2580.
- [22] A.V. Zemskov, G.N. Rodionova, Y.G. Tuchin, V.V. Karpov, *Zh. Prikl. Spektrosk.* 49 (1988) 581.
- [23] H.-L. Li, Y. Ujihara, S. Tanaka, T. Yamashita, K. Horie, *J. Radioanal. Nucl. Chem.* 210 (1996) 543.
- [24] A. Natansohn, P. Rochon, X. Meng, C. Barrett, T. Buffeteau, S. Bonenfant, M. Pezolet, *Macromolecules* 31 (1998) 1155.
- [25] Z. Sekkat, M. Dumont, *Appl. Phys. B* 54 (1992) 486.
- [26] T. Ikeda, O. Tsutsumi, *Science* 268 (1995) 1873.
- [27] A. Shishido, O. Tsutsumi, A. Kanazawa, T. Shiono, T. Ikeda, N. Tamai, *J. Am. Chem. Soc.* 119 (1997) 7791.
- [28] S. Hvilsted, F. Andruzzi, C. Kulinna, H.W. Siesler, P.S. Ramanujam, *Macromolecules* 28 (1995) 2172.
- [29] J.G. Radziszewski, J. Michl, *J. Chem. Phys.* 82 (1985) 3527.
- [30] T. Asano, T. Okada, *J. Org. Chem.* 49 (1984) 4387.
- [31] H.-L. Li, Y. Ujihara, A. Nanasawa, *J. Radioanal. Nucl. Chem.* 210 (1996) 533.
- [32] D. Anwand, W. Müller, B. Strehmel, K. Schiller, *Makromol. Chem.* 192 (1991) 1981.